The Development of Statistical Volcanology: A Personal Experience

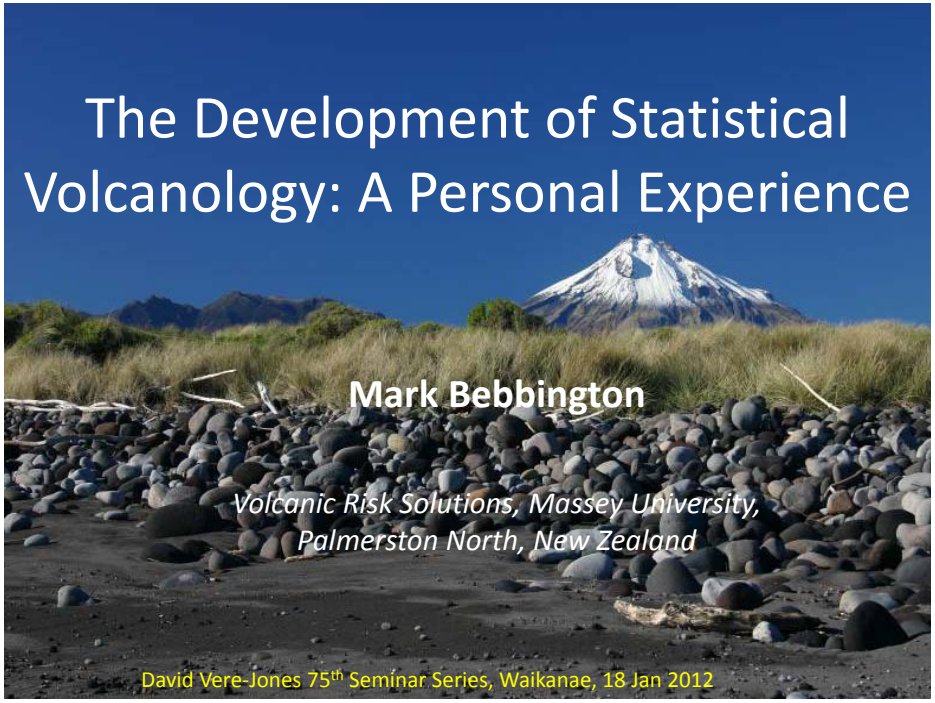

Mark Bebbington

Volcanic Risk Solutions, Massey University, Palmerston North, New Zealand

David Vere-Jones 75th Seminar Series, Waikanae, 18 Jan 2012

What about Statistical Seismology then?

Probabilistic Sesimic Hazard Analysis (PSHA)

- From PGA to failure: engineering
- From event to PGA: interesting, data?
- Location, size and mechanism of event
  - Earthquakes occur in 8-D (t,x,y,z,strike,dip,rake,slip)
- Event occurrence
  - Aftershocks
    - Omori – ETAS, 118 years of evolution?
  - Mainshocks
    - CFS
      - Worked(?) for strongly linear N Anatol. fault
      - Elsewhere?
    - Time/size predictable, other regression methods
    - Stress-release models

All require identification of spatial structure

Linked Stress Release Model (Japan)

Lu et al. (1999)

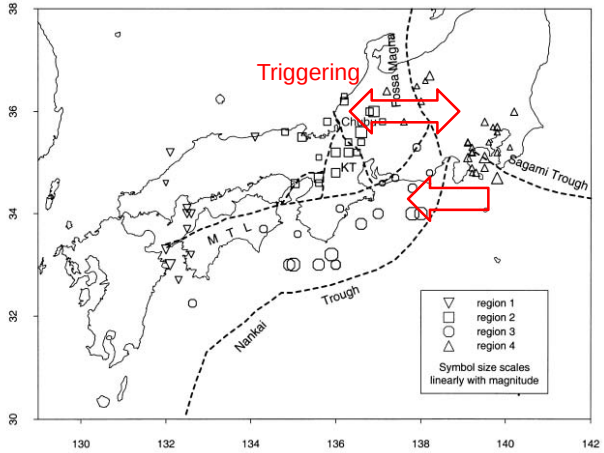

Fig. 1. The epicenter distribution of major earthquakes with magnitude $M \geq 6.5$ (Utsu's catalog). Regions are based on major tectonic features as shown; MTL is the Median Tectonic Line, KT the Kinki triangle, and Chubu refers to the district.

Linked Stress Release Model (Taiwan)

Bebbington and Harte (2001)

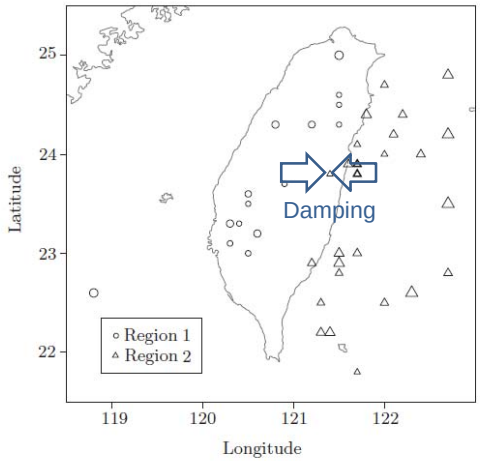

FIGURE 1: The seismic zone around Taiwan, with the epicentres and magnitudes ($M \geq 6.5$) of events from the Taiwan earthquake catalog, 1902–1996. Symbol size scales with magnitude.

Linked Stress Release Model (GJI 2003)

Bebbington and Harte (2003)

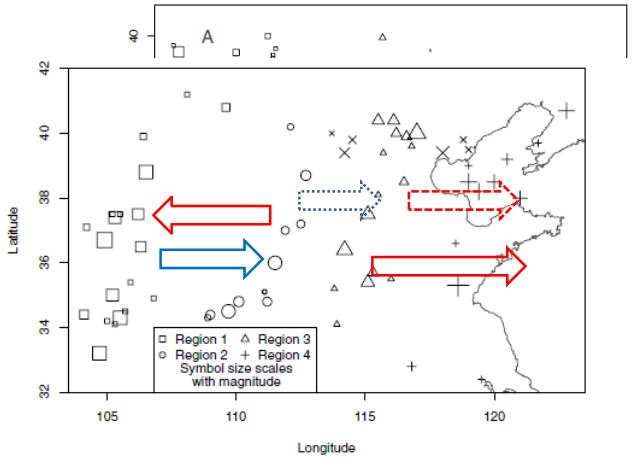

Figure 4. North China earthquakes 1480–1996. The crosses mark events that are allocated to different regions in the different data sets.

Longitude

Figure 1. Persian earthquakes, 1780–1994. The region boundaries are those of Zheng & Vere-Jones (1994).

Catch 22

In order to quantify spatial (etc. etc.) dimension(s) we need to either:

a) Impose an exogenous spatial structure such as
   i. Regions
      1. But what is a region?
      2. How is it chosen?
      3. Do two events that are 10km or 1000km apart really have the same effects because the regions are the same?
   ii. Faults
      1. What is a fault?
      2. Do earthquakes always occur on (known?) faults?

b) Have a lot more data, which means
   i. Bringing in aftershocks
      1. Is any more information gained?
      2. Are we back to modelling the Omori law?
   ii. Simulating data
      1. Supercomputing ....

BUT! Volcanoes don't move around (much)

Volcanic Data

Of course, there are another set of problems ...

Such as completeness:

• Globally, the observance probability rises from 10% in 1500 to 100% in 1980 (Guttorp and Thompson, 1991).

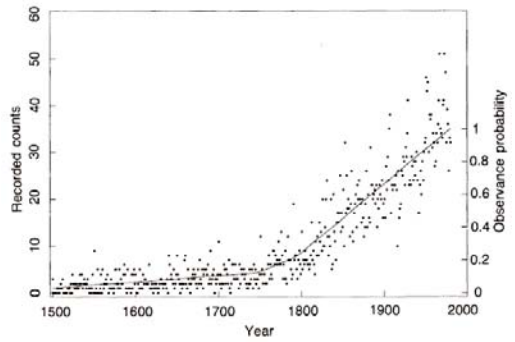

BUT

– some volcanoes are much better observed

- Big eruptions are much better observed

- what is an eruption?

What is an Eruption?

- Events ranging from individual explosions to eruptive periods lasting centuries
  - Includes quiet periods of up to 3 months
  - Often 'stop' dates go unrecorded.
- 'Historical' eruptions
  - Presence of observers, monitoring, weather
- 'Pre-historical' eruptions
  - Dated, radio-carbon (to 50ka, with error ~ 25 to 1000 yr), K-Ar dating (from 50ka, with error ~ 10 to 100 ka).
- VEI (Volcanic Explosivity Index)
  - a logarithmic 'size' assigned to historical eruptions on the basis of: explosion size; volume; column height; classification; duration; ...
  - all non-explosive eruptions (some very large) are VEI 0

Eruption size

	0	1	2	3	4	5	6	7	8
General Description	Non-Explosive	Small	Moderate	Moderate-Large	Large	Very Large			
Volume of Tephra (m^3)	$1x10^4$	$1x10^6$	$1x10^7$	$1x10^8$	$1x10^9$	$1x10^{10}$	$1x10^{11}$	$1x10^{12}$	
Cloud Column Height (km) Above crater / Above sea level	<0.1	0.1-1	1-5	3-15	10-25	>25			
Qualitative Description	"Gentle,"	"Effusive"	"Explosive"		"Cataclysmic," "Severe,"	"paroxysmal," "violent,"	"terrific"	"colossal"	
Eruption Type	Hawaiian	Strombolian	Vulcanian		Plinian		Ultra-Plinian		
Duration (continuous blast)	<1 hour		1-6 hrs	6-12 hrs	>12 hrs				
CAVW max explosivity (most explosive activity listed in CAVW)	Dome or mudflow	Lava flow	Phreatic		Explosion or Nuée ardente				
Tropospheric Injection	Negligible	Minor	Moderate	Substantial					
Stratospheric Injection	None	None	None	Possible	Definite	Significant			
Eruptions (total in file)	755	963	3631	924	307	106	46	4	0

VEI	Tephra Volume (km3)	Example
0	Effusive	Masaya (Nicaragua), 1570
1	>0.00001	Poás (Costa Rica), 1991
2	>0.001	Ruapehu (New Zealand), 1971
3	>0.01	Nevado del Ruiz (Colombia), 1985
4	>0.1	Pelée (West Indies), 1902
5	>1	Mount St. Helens (United States), 1980
6	>10	Krakatau (Indonesia), 1883
7	>100	Tambora (Indonesia), 1815
8	>1000	Yellowstone (United States), Pleistocene

A Prediction?

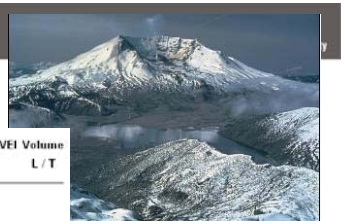

Area of Activity	Start Year	Start MoDy	Stop Year	Stop MoDy	Eruptive Characteristics	VEI	Volume L / T
North flank	1857	04..	....	....	---- ---- x--- ---- ----	2	
North flank	1854	02..	1854	04..	-x-- ---- x--- ---- ----	2	

"The repetitive nature of the eruptive activity at Mt St Helens during the last 4000 years, with dormant intervals typically of a few centuries or less, suggests that the current quiet period will not last a 1000 years. Instead, an eruption is likely within the next hundred years, possibly before the end of this century"

- Crandell et al., "Mt St Helens volcano: Recent and future behavior". Science 187:438-441, ***1975***

Mt St Helens erupted in 1980, having been quiescent since 1857

A Model?

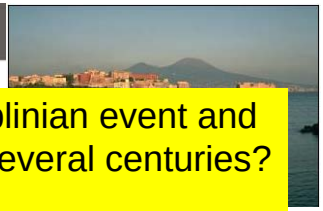

VEI > 3

Cycles initiated by (sub-)plinian event and terminated by repose of several centuries?

Area of Activity		Start Year	Start MoDy	Stop Year	Stop MoDy	Eruptive Characteristics	VEI	Volume L / T
Summit and upper flanks		1875	1218	1906	0422	x-x- ---- xx-- x--- xxx-	4?	7 / 8
Summit, SW and S flanks		1631	1215	1632	0131?	x-x- ---- xx-- ---- xxxx	5?	– / 9
		0968	1201p	....	....	x--- ---- x--- x---?--	4	– / 8
		0685	02..	0685	03..	x--- ---- x---?---x--	4	– / 8
		0536	....	....	....	x--- ---- x--- ---- -x?-	4?	
		0472	1105	0472	1106?	x-?- ---- xx--?---xx-	5	– / 9
(Pompeii eruption)		0079	0824	0079	0828a	x--- ---- xx-- ---- xxxx	5?	– / 9
(AP3 tephra layer)	G	-0890v	....	....	....	x--- ---- x--- ---- -xx-	4	– / 8
Piano delle Ginestre (AP2 tephra layer)	G	-1430y	....	....	....	x--- ---- x--- ---- ----	4	– / 8
Piano delle Ginestre (AP1 tephra layer)	G	-1800x	....	....	....	x--- ---- x--- ---- ----	4	– / 8
Piano delle Ginestre (Avellino eruption)	G	-1900w	....	....	....	x--- ---- xx-- ---- xxx-	5	– / 9
(Pomici e Proietti eruption)	C	-3580?	....	....	....	x--- ---- x--- ---- --x-		
(Mercato-Ottaviano eruption)	C	-5960v	....	....	....	x--- ---- xx-- ---- --x-	5	– / 9

A simple question: Do eruptions cluster in time?

For a polygenetic volcano, does an eruption make further eruptions in the near future:

A. More likely?
   - Clustering

B. Less likely?
   - (Quasi-)Periodicity

Many investigations (renewal models, fractal analysis, chaos theory,...) have concluded that either (or both!) occur

Stationarity

All the approaches considered assume that the eruption onset process is statistically stationary.

Nonstationarity confounds with clustering leading to overestimation of the latter.

Increasing (with time) observation probability means that the data may not be stationary, even if the process is.

What about for the best data?

→ Bebbington (2010)

Twelve angry volcanoes

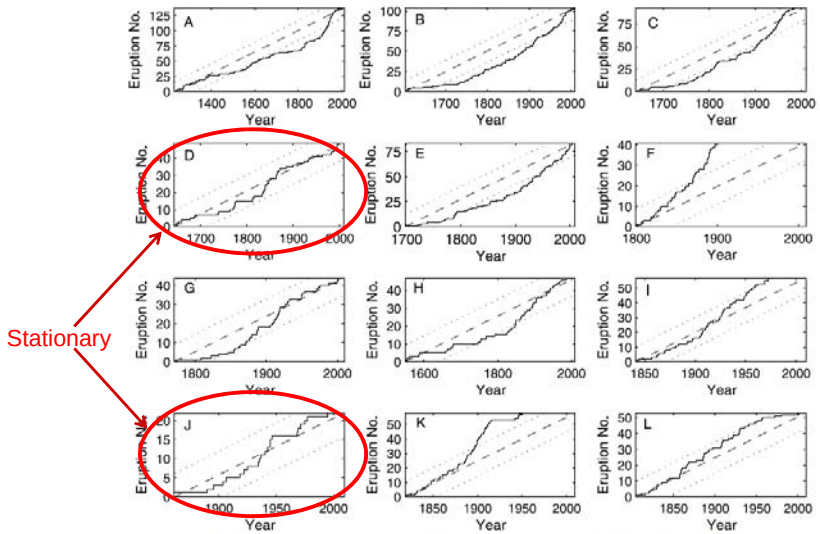

Figure 2. Cumulative number of eruptions (solid line), average rate (dashed line) and 95% confidence band for a stationary rate process (dotted lines). (a) Aso, (b) Etna, (c) Fourmaise, (d) Gamalama, (e) Kliuchevskoi, (f) Lamongan, (g) Murapi, (h) Merapi, (i) Ngauruhoe, (j) Ruapehu, (k) Semeru, (l) Tengger.

Some stochastic (point process) models

Let N(s,t) = number of onsets in time interval (s,t). The *point process intensity* is

$$\lambda(t) = \lim_{\Delta t \downarrow 0} \frac{\Pr(N(t, t+\Delta t) = 1)}{\Delta t}$$

ie, the probability of an event in $(t,t+\Delta t)$ is approx. $\lambda(t)\Delta t$

- *Poisson process*, $\lambda(t) = \nu$, a constant
- *Renewal process*, $\lambda(t) = \frac{f(t-s)}{1-F(t-s)}$ where the previous event occurred at s
  - *Weibull renewal process*, $\lambda(t) = \eta\nu(\nu(t-s))^{\eta-1}$ so $\eta < 1$ (> 1) results in clustering (quasi-periodicity)
- *Nonhomogeneous Poisson (Weibull) process* $\lambda(t) = \kappa\theta^{-\kappa}t^{\kappa-1}$ which is monotonically increasing (decreasing) for $\kappa > 1$ (< 1).

Trend renewal process (Lindqvist et al 2003)

Given:

an increasing function $\Psi(t)$ and a renewal distribution F,

the trend renewal process (TRP) is defined by:

$r_i = \Psi(t_i) - \Psi(t_{i-1})$ being IID RVs with distribution F, where t_i are the event times.

➢ Let $\Psi(t) = \int_0^t \psi(s)ds$ where $\psi(s)$ is a nonnegative function

➢ Identifiability is dealt with by making $\Psi(T) = T$, the length of the observation window.

TRP: Special Cases

$\psi(t) = 1$: stationary renewal process, distribution F

$F(r) = 1 - \exp(-\nu r)$: nonhomogeneous Poisson process, intensity $\nu\psi(t)$

Hence choose:

and $F(r) = 1 - \exp\left(-(\nu r)^{\eta}\right)$

$\psi(t) = \mu + (1-\mu)g(t)$, where $0 < \mu < 1$

to allow for two end members: a stationary Weibull renewal process ($\mu = 1$) and a NHPP ($\eta = 1$).

TRP: Nonstationarity

Increasing/decreasing activity: $\psi(t) = \mu + (1-\mu)\kappa\left(\frac{t}{T}\right)^{\kappa-1}$

(*Weibull TRP*) with 4 parameters

Wax-and-wane: $\psi(t) = \mu + \frac{(1-\mu)T\beta^{\alpha}t^{\alpha-1}}{\exp(\beta t)\Gamma(\beta T,\alpha)}$, where $\Gamma(\beta T,\alpha) = \int_0^{\beta T} u^{\alpha-1}e^{-u}du$

(*Gamma TRP*) with 5 parameters

Cycles: $\psi(t) = \mu + (1-\mu)\left(\phi\kappa\left(\frac{t}{T}\right)^{\kappa-1} + (1-\phi)\left[1+\sin\left(\frac{\omega 2\pi t}{T}+\rho\right)\right]\right)$

(*Cyclic TRP*) with 7 parameters

TRP: MLE / AIC

The likelihood is

$$L = \left(1 - F\left[\Psi(T) - \Psi(t_n)\right]\right)\prod_{i=1}^{n} f\left[\Psi(t_i) - \Psi(t_{i-1})\right]\psi(t_i)$$

with onsets observed at $t_1 < t_2 < \ldots < t_n$ for $0 < t_i < T$

Models compared using

$$AIC = -2p + 2\log L,$$

for p fitted parameters, allowing us to avoid overfitting and identify the 'real' features.

Best Models

Stationary Renewal Proc.

Inc/Dec trend TRP

Wax-and-wane TRP

Cyclic TRP

Table 1. Volcanoes and Model AICs[a]

Volcano	Start Year	n	AIC_0	AIC_W	AIC_G	AIC_C
Aso	1230.0	138	−742.2	−724.6	−726.6	*−712.3*
Etna	1603.5	104	−487.6	*−461.5*	−462.5	−463.7
Fournaise	1640.5	93	−437.8	−425.8	−423.8	*−418.4*
Gamalama	1643.5	49	*−292.7*	−295.6	−296.3	−293.8
Kliuchevskoi	1697.5	84	−389.2	*−363.2*	−365.2	−364.7
Lamongan	1799.5	41	−196.2	−200.1	*−179.5*	−203.0
Marapi	1770.5	44	−234.8	−231.1	*−223.4*	−231.5
Merapi	1548.5	47	−306.5	−304.7	*−295.1*	−297.5
Ngauruhoe	1841.5	57	−235.7	−238.9	*−225.6*	−234.2
Ruapehu	1861.1	22	−127.6	−129.4	*−123.1*	−128.2
Semeru	1818.9	58	−241.6	−245.6	*−220.3*	−241.5
Tengger	1804.7	53	−249.7	−253.6	*−242.2*	−256.9

[a]Italic values indicate the preferred model for the given volcano.

Increasing Activity

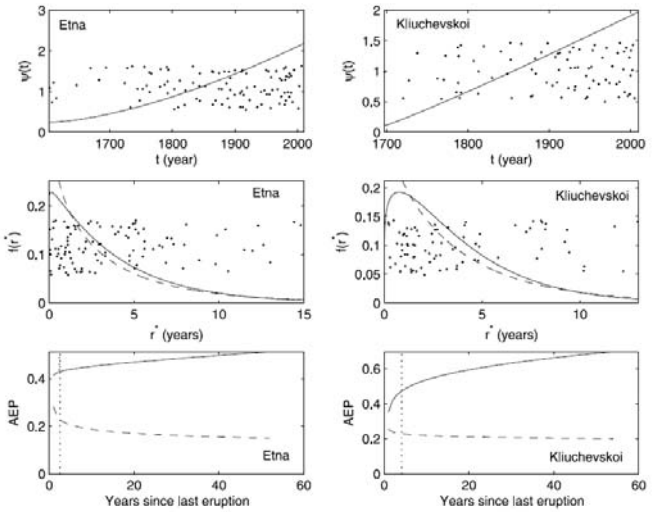

Figure 3. (top) Fitted Weibull TRP $\psi(t)$ from (7), (middle) $f(r^*)$ from (3), and (bottom) estimated AEP for the next eruption with VEI ≥ 2 for Etna and Kliuchevskoi. Data points indicated by dots are the onset dates (Figure 3, top) and scaled interonset times (Figure 3, middle). Both are jittered vertically. The dashed lines in Figures 3 (middle) and 3 (bottom) are the corresponding quantities from the stationary renewal process ($\psi(t) = 1$).

Wax-and-wane

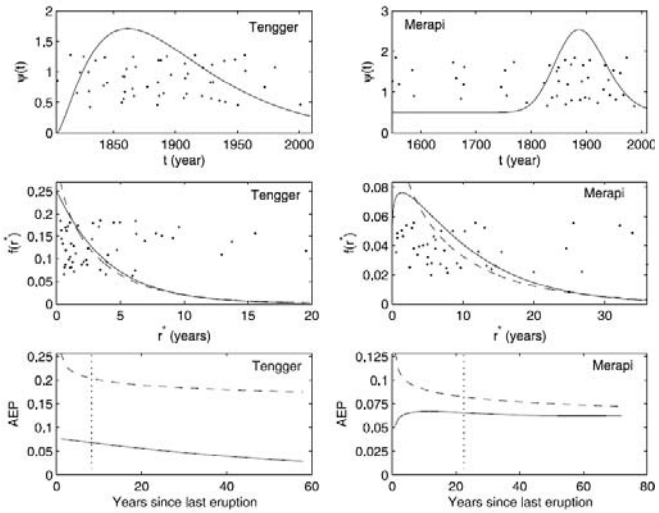

Figure 4. (top) Fitted gamma TRP $\psi(t)$ from (8), (middle) $f(r^*)$ from (3), and (bottom) estimated AEP for the next eruption with VEI ≥ 2 for Tengger and Merapi. Data points indicated by dots are the onset dates (Figure 4, top) and scaled interonset times (Figure 4, middle). Both are jittered vertically. The dashed lines in Figures 4 (middle) and 4 (bottom) are the corresponding quantities from the stationary renewal process ($\psi(t) = 1$).

Cycles

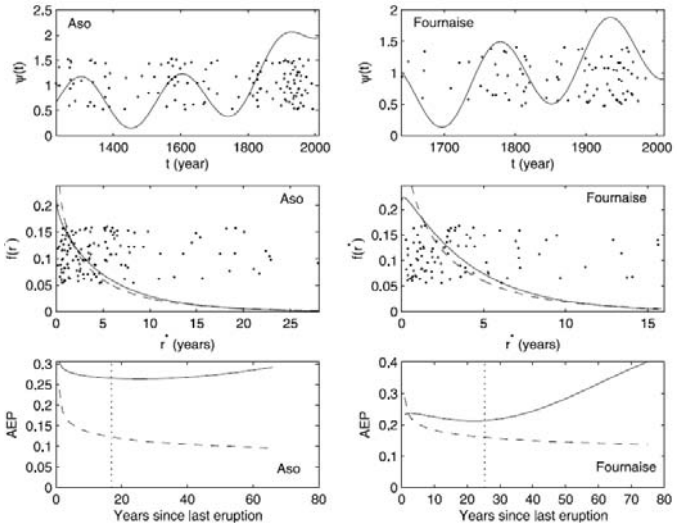

Figure 5. (top) Fitted cyclic plus trend TRP $\psi(t)$ from (9), (middle) $f(r^*)$ from (3), and (bottom) estimated AEP for the next eruption with VEI ≥ 2 for Aso and Fournaise. Data points indicated by dots are the onset dates (Figure 5, top) and scaled inter-onset times (Figure 5, middle). Both are jittered vertically. The dashed lines in Figures 5 (middle) and 5 (bottom) are the corresponding quantities from the stationary renewal process ($\psi(t) = 1$).

What about the clustering???

Red = preferred model
Green = Clustered
Blue = Quasiperiodic

Table 5. Clustering Parameters[a]

Volcano	η_0	ν_0	η_W	ν_W	η_G	ν_G	η_C	ν_C
Aso	0.81 ± 0.08	0.20 ± 0.04	0.88 ± 0.09	0.19 ± 0.03	0.81 ± 0.09	0.20 ± 0.03	*0.96 ± 0.10*	*0.18 ± 0.03*
Etna	0.86 ± 0.10	0.28 ± 0.05	*1.03 ± 0.11*	*0.25 ± 0.04*	1.03 ± 0.11	0.25 ± 0.04	1.05 ± 0.11	0.25 ± 0.04
Fournaise	0.85 ± 0.10	0.28 ± 0.06	0.91 ± 0.09	0.26 ± 0.05	0.94 ± 0.11	0.26 ± 0.05	*1.03 ± 0.14*	*0.25 ± 0.04*
Gamalama	*0.86 ± 0.16*	*0.14 ± 0.04*	0.86 ± 0.15	0.14 ± 0.03	0.88 ± 0.18	0.14 ± 0.04	0.94 ± 0.18	0.13 ± 0.03
Kliuchevskoi	0.95 ± 0.10	0.27 ± 0.05	*1.17 ± 0.14*	*0.25 ± 0.03*	1.17 ± 0.19	0.25 ± 0.03	1.21 ± 0.14	0.25 ± 0.03
Lamongan	0.68 ± 0.13	0.29 ± 0.12	0.69 ± 0.13	0.28 ± 0.08	*0.95 ± 0.17*	*0.19 ± 0.04*	0.71 ± 0.14	0.27 ± 0.12
Marapi	0.84 ± 0.16	0.20 ± 0.06	0.90 ± 0.17	0.19 ± 0.04	*0.97 ± 0.17*	*0.18 ± 0.05*	0.98 ± 0.19	0.18 ± 0.04
Merapi	0.89 ± 0.13	0.11 ± 0.03	0.97 ± 0.18	0.10 ± 0.03	*1.12 ± 0.07*	*0.96 ± 0.06*	1.12 ± 0.18	0.10 ± 0.02
Ngauruhoe	0.85 ± 0.15	0.37 ± 0.09	0.85 ± 0.12	0.37 ± 0.08	*1.00 ± 0.19*	*0.33 ± 0.07*	0.88 ± 0.15	0.36 ± 0.09
Ruapehu	0.90 ± 0.23	0.15 ± 0.06	0.92 ± 0.26	0.15 ± 0.05	*1.04 ± 0.32*	*0.14 ± 0.04*	1.07 ± 0.35	0.14 ± 0.04
Semeru	0.75 ± 0.13	0.38 ± 0.09	0.75 ± 0.12	0.38 ± 0.11	*0.98 ± 0.15*	*0.30 ± 0.07*	0.81 ± 0.12	0.35 ± 0.08
Tengger	0.91 ± 0.18	0.27 ± 0.07	0.92 ± 0.14	0.27 ± 0.07	*1.01 ± 0.20*	*0.25 ± 0.06*	0.91 ± 0.17	0.27 ± 0.07

[a]Italic values indicate the preferred model for the given volcano.

Shift from clustered towards quasiperiodic once change in activity level is allowed for!

Sensitivity to start date and incompleteness

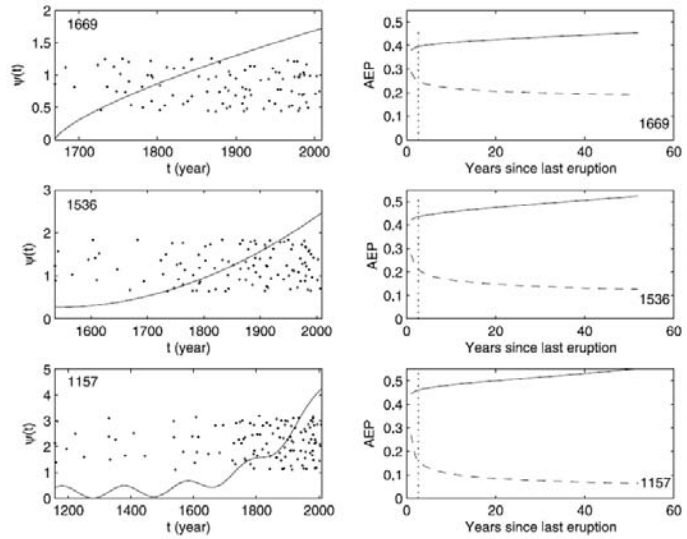

Figure 7. Sensitivity analysis for Etna to start date (1669, 1536, 1157, see Figure 3 for 1600). (left) Best fitted TRPs $\psi(t)$. Data points indicated by dots are the onset dates, jittered vertically. (right) Estimated AEP for the next eruption with VEI ≥ 2.

Best Model (including nuisance parameters)

η, ϕ, μ are potential nuisance parameters – if = 0 or 1, they do not exist in the model

Table 7. Best AIC Models and Forecasts[a]

Volcano	Model	Number of Parameters	AIC	Quantiles (u) of $P(t_{n+1} > u \mid P(t_{n+1} > 2009.2)$ 95th	UQ	Median	LQ	5th
Aso	Cyclic, $\eta = 1$	6	−710.8	2009.4	2010.1	2011.3	2011.4	2013.3	2018.0
Etna	Weibull, $\eta = 1$	3	−459.6	2009.3	2009.8	2010.3	2010.5	2011.7	2014.6
Fournaise	Cylic, $\eta = 1$, $\mu = 0$	5	−414.5	2009.5	2010.5	2010.8	2012.3	2015.2	2021.8
Gamalama	Cyclic, $\eta = 1$, $\phi = 0$	5	−290.0	2009.5	2010.8	?	2012.9	2016.4	2024.2
Kliuchevskoi	Weibull, $\mu = 0$	3	−361.3	2009.4	2010.0	2010.8	2011.3	2012.0	2014.6
Lamongan	Gamma, $\eta = 1$, $\mu = 0$	3	−175.7	2010.2	?	2015.1	2024.6	2042.8	2082.5
Marapi	Gamma, $\eta = 1$, $\mu = 0$	3	−219.5	2009.7	?	2012.0	2016.0	2023.7	2046.8
Merapi	Gamma, $\eta = 1$	4	−293.9	2010.1	2010.8	2014.1	2021.1	2033.7	2064.1
Ngauruhoe	Gamma, $\eta = 1$	4	−223.6	2009.6		2011.2	?	2014.0	2018.8	2030.1
Ruapehu	Gamma, $\eta = 1$, $\mu = 0$	3	−119.2	2010.0	?	2013.9	2020.7	2033.4	2065.1
Semeru	Gamma, $\eta = 1$, $\mu = 0$	3	−216.3	2010.1		2014.4	2022.9	2039.7	2075.1
Tengger	Gamma, $\eta = 1$, $\mu = 0$	3	−238.3	2010.0	2010.9	2013.5	2020.2	2033.8	2093.2

[a]LQ and UQ are lower and upper quantiles, respectively.

The 1967 eruption of Semeru is continuing

Mt Taranaki: Likelihood of an eruption

(Turner et al 2008, 2009)

Cores from Umutekai (104 tephras) and Rotokare (45 tephras)
Also 23 `near-source' tephras

How do we extract the eruptive record?

Prevailing wind direction

Recovering Ages from Depths

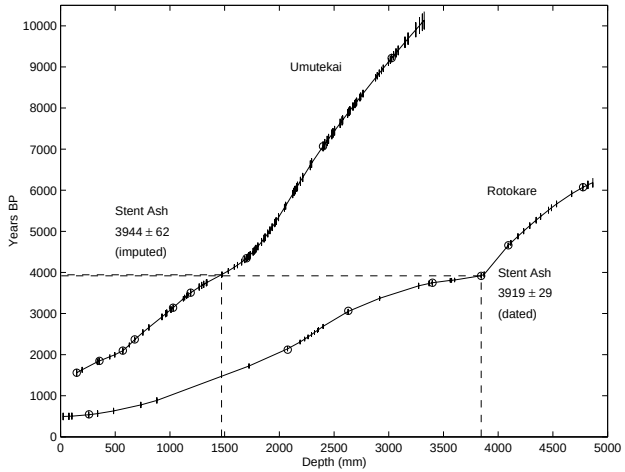

We fit a spline to the known depth/age pairs and impute the remaining ages.

<u>Umutekai</u>

104 tephras, c. 1550BP – 10100BP

<u>Rotokare</u>

45 tephras, c. 500BP – 6200BP

<u>Near-source</u>

23 tephras, c. 90BP – 2200BP

Overlapping ages

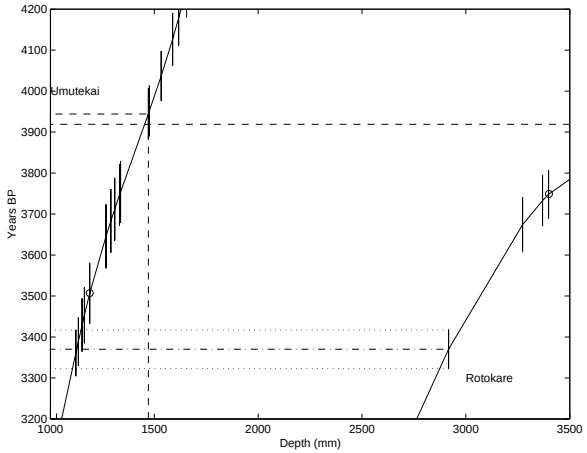

Blown up section of the depth-date curves

- This Rotokare event overlaps 4 Umutekai events.
- Which, if any, is the `same' event?
- Need `best' matches
- Check via geochemistry

Identifying Common Events

Calculate distance between two tephra from different sources as

$$d_{1,2} = \frac{|m_1 - m_2|}{\sqrt{s_1^2/2 + s_2^2/2}} \sim N(0,1)$$

This identifies candidates, e.g., those pairs at a distance less than 2.

- Assign mutually closest pairs to each other
- Then assign other matches on the basis of temporal distance and stratigraphy
- 25 matches between Rotokare and Umutekai dates 2250-6250 BP

All candidates listed, closest in parentheses, and final match in bold

Closest neighboring tephras. Left columns are closest Umutekai tephra for the given Rotokare tephra, right columns the reverse.

Rotokare tephra no.	Umutekai tephra no.	Umutekai tephra no.	Rotokare tephra no.
10	**7**	**7**	**10**
12	**9**	**9**	**12**
14	10	**10**	14 (**15**) 16
15	**10**	**11**	17 (**18**)
16	10	13	19
17	11	**14**	**19**
18	**11**	15	19
19	13 (**14**) 15	**17**	**20**
20	(**17**) 18	18	20
21	22 (**23**) 24	22	21
22	23 *24* (25) 26	**23**	(**21**) 22 23
23	23 24 (**25**) 26	*24*	21 (*22*) 23
24	25 (26)	**25**	22 (**23**) 24
25	26	*26*	22 (23) *24* 25
27	(27) 28	*27*	27 (28)
28	27 (**28**)	**28**	27 (**28**)
29	**43**	**43**	**29**
30	**44**	**44**	**30**
31	45 (**46**) 47	45	31
32	47 (**48**)	**46**	**31**
33	(**49**) 50	47	31 (32)
34	51 (**52**) 53	**48**	**32**
35	**53**	**49**	**33**
36	54	50	33
37	(**54**) 55	51	34
38	**55**	**52**	**34**
39	(**56**) 57 58	**53**	34 (**35**)
40	58 59 60 (**61**) 62	**54**	36 (**37**)
41	60 61 (**62**) 63	**55**	37 (**38**)
42	62 (**63**)	**56**	**39**
		57	39
		58	(39) 40
		59	40
		60	(40) 41
		61	(**40**) 41
		62	40 (**41**) 42
		63	41 (**42**)

Eruption Coverage

Number of events by source(s) and age (years BP)

	96-450	450-1500	1500-2250	2250-6250	6250-10150
NS only	11	4			
NS + R		4	1		
NS + U			3		
R only		4	1	7	
R + U				24	
U only			5	30	41

A record with 136 events, and uneven coverage

Note that of the events in 2250-6250, 48% are in U only, 11% in R only and 41% in both – a third (or fourth?) source might produce more events, and there are certainly missing events in 6250-10150

Moreover, these matches are on the basis of date alone - Can we check the assignments through geochemistry?

Geochemistry: 75-88% confirmed

We have geochemistry for 15 of the 25 common events in 2250-6250, plus the Stent Ash is a match

11 of these overlap, one is inconclusive (1 datum) and 3 do not

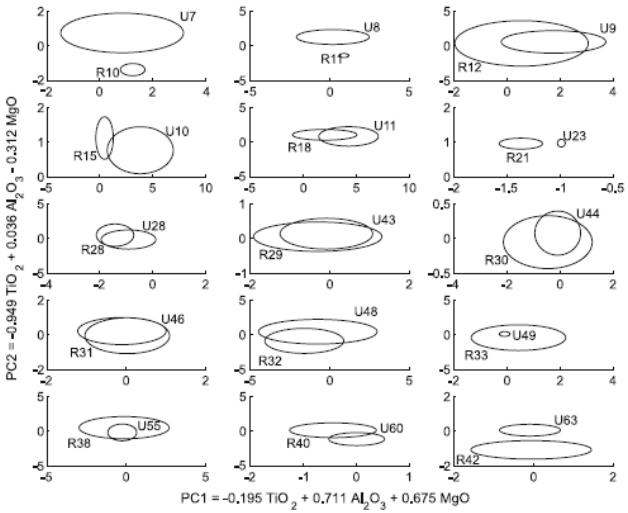

Leads to better matches at the 'ends'

Next Step?: Combined Data

Problem: Data is still incomplete, but now also inhomogeneous.

Hence use only post-6250 data to formulate probabilistic hazard model.

We average dates from multiple sources and combine uncertainties

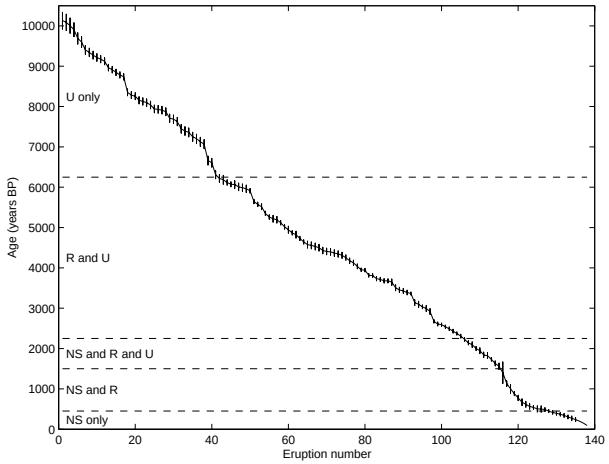

Renewal Models

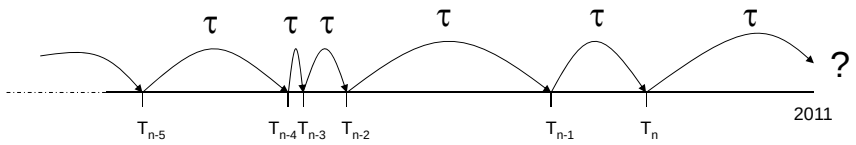

- Assumption is that interval lengths τ are independent, identically distributed.
  - Unlikely for complete record, but sedimentary data likely to be more homogeneous ☺
- Sedimentary data will tend to be under-dispersed in time.
  - Try Weibull, Lognormal distributions

Fitted Model

NS + U, post-10150

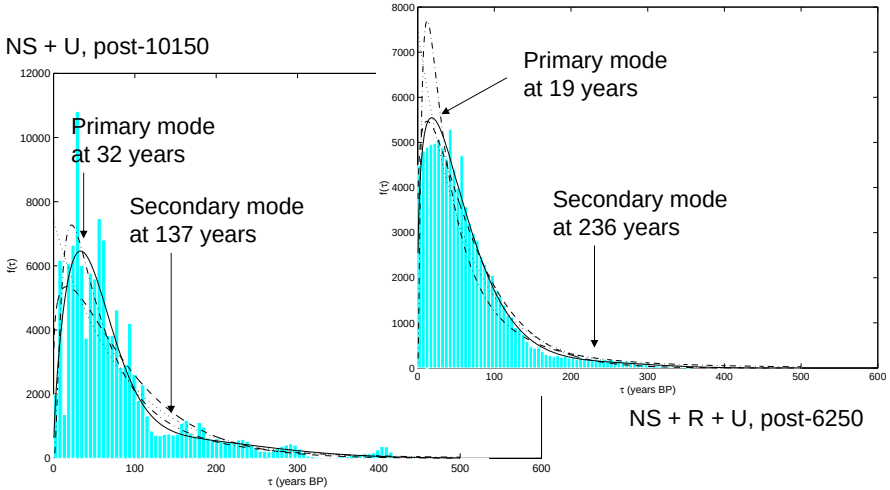

NS + R + U, post-6250

Dotted = exponential, dot-dash = lognormal, dashed = Weibull, solid = mixture of Weibulls (ΔAIC > 2)

Forecast: NS + U, post-10150 data

50 year probability of an eruption is

0.37 for the 1854 scenario,

0.48 for the 1755 scenario

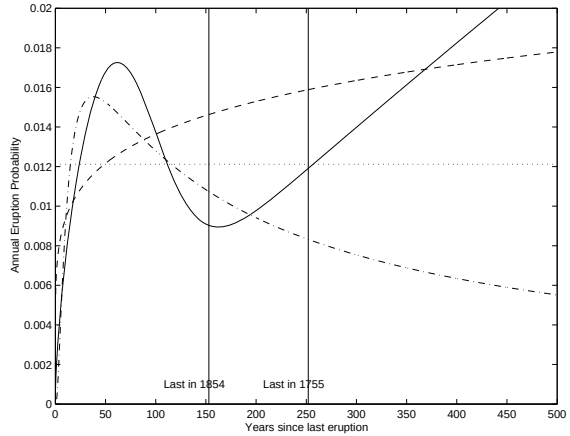

Dotted = exponential, dot-dash = lognormal, dashed = Weibull, solid = mixture of Weibulls

Forecast: NS + R +U, post-6250 data

50 year probability of an eruption is 0.52 (+0.15) for the 1854 scenario, 0.66 (+0.18) for the 1755 scenario

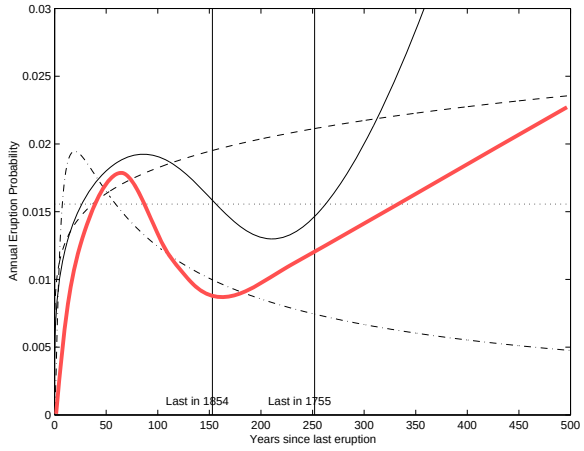

Dotted = exponential, dot-dash = lognormal, dashed = Weibull, solid = mixture of Weibulls
Red curve is NS+U, post-10150 model

Volcanic Regimes

Flank eruptions at Mt Etna

Bebbington (2007)

Table 2. Flank eruptions at Mount Etna, 1601–2006. Durations are in days.

Date	Duration	VEI	Date	Duration	VEI
2004.9.7	190	1	1874.8.29	3	2
2002.10.26	95	3	1865.1.30	150	2
2001.7.17	24	2	1852.8.20	281	2
1991.12.14	473	2	1843.11.17	12	2
1989.9.11	29	2	1832.10.31	23	2
1986.10.30	123	2	1819.5.27	71	2
1985.12.19	13	1	1811.10.27	202	2
1985.3.8	128	1	1809.3.27	14	2
1983.3.28	132	1	1802.11.15	4	2
1981.3.17	7	2	1792.5.25	367	3
1979.7.16	414	3	1792.3.15	71	2
1978.4.29	216	2	1780.4.20	57	2
1975.2.24	187	1	1766.4.27	194	2
1974.1.30	59	2	1763.6.18	85	3
1971.4.5	69	2	1763.2.6	33	2
1950.11.25	373	2	1758.11.3	272	2
1949.12.2	4	2	1755.3.9	7	3
1947.2.24	15	1	1702.3.8	62	1
1942.6.30	2	2	1689.3.14	62	1
1928.11.2	19	1	1682.9.1	45	2
1923.6.17	32	2	1669.3.11	123	3
1918.11.30	2	1	1651.1.17	911	1
1911.9.10	13	1	1646.11.20	59	2
1910.3.23	27	2	1643.2.20	9	1
1908.4.29	3	2	1634.12.19	1226	1
1892.7.9	174	2	1614.7.1	3654	2
1886.5.18	21	3	1610.2.6	191	2
1883.3.22	3	2	1607.6.28	370	2
1879.5.26	13	3			

Table 10. Flank eruptions at Mount Etna, 1601–2006 (catalogue 2). Durations are in days.

Date	Duration	Date	Duration
2004.9.7	190	1892.7.11	171
2002.10.27	94	1886.5.18	22
2001.7.12	23	1883.3.22	3
1991.12.14	474	1879.5.26	11
1989.9.27	13	1874.8.29	3
1986.10.30	123	1865.5.30	31
1985.12.25	7	1852.8.20	280
1985.3.10	126	1843.11.17	12
1983.3.28	132	1832.11.1	21
1981.3.17	7	1819.5.27	66
1979.8.3	7	1811.10.28	179
1978.11.23	8	1809.3.28	13
1978.8.25	6	1802.11.15	4
1978.4.29	38	1792.6.1	302
1975.11.29	406	1792.5.11	2
1975.2.24	187	1780.4.20	42
1974.3.11	19	1766.4.27	194
1974.1.30	19	1763.6.20	84
1971.4.5	69	1763.2.5	33
1950.11.25	372	1759.5.1	93
1949.12.2	4	1755.3.9	6
1947.2.21	18	1702.3.8	5
1942.6.30	2	1689.3.14	62
1928.11.3	18	1669.3.11	122
1923.6.16	31	1651.1.16	730
1918.11.29	1	1646.11.20	58
1911.9.9	14	1634.12.19	1224
1910.3.23	37	1614.7.1	3650
1908.4.29	1	1610.2.6	159

Hidden Markov Models

- We have $X_k \in S$ hidden states,

a transition matrix A, where $a_{ij}=Pr(X_k=j|X_{k-1}=i)$, and observations o_k, with density $f_x(o_k;\theta_x|X_k=x)$

- These can be fitted by way of the EM algorithm.

- The forward-backward equations also estimate the probability that the hidden chain is in each state at each time (Cf. the Viterbi Algorithm, which identifies the most likely sequence of states)

Discrete Time HMM

Table 4. Onset models for Mount Etna.

Model	S	AIC	λ	A		State	Sojourn (yr)	Mean eruptions per year
Empirical	1	−182.77	1			1	∞	0.1425
Eq. (14)	2	−187.04	0.98	0.02		1	203.3	0.116
			0.50	0.50		2	9.9	0.509
	3	−196.06	0.98	0	0.02	1	287.4	0.111
			0.29	0	0.71	2	5	0.279
			0	1	0	3	5	0.525
Poisson	1	−180.07	1			1	∞	0.1425
Eq. (15)	2	−183.69	0.97	0.03		1	193.1	0.113
			0.27	0.73		2	18.7	0.382
	3	−193.85	0.70	10^{-4}	0.30	1	16.4	0
			0.03	0.97	0	2	195.3	0.121
			0	0.24	0.76	3	21.2	0.381

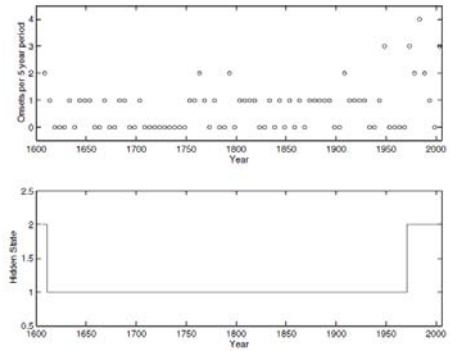

Figure 2. Mount Etna: optimal hidden path for the discrete Poisson HMM.

Continuous HMM

Discretize by considering interevent times as continuous variables from a discrete time chain

Table 5. Interonset models for Mount Etna.

Model	S	AIC	A (Q for the MMPP)			State	Sojourn (eruptions)	Interonset time (d) Mean	*SD*
Exponential	1	−994.28	1			1	∞	2591	2591
Eq. (16)	2	−996.36	1	0		1	∞	908	908
			0.02	0.98		2	43.10	3107	3107
	3	−1007.32	1	0	0	1	∞	908	908
			0	0.03	0.97	2	1.03	975	975
			0.02	0	0.98	3	42.02	3162	3162
Weibull	1	−996.22	1			1	∞	2594	2531
Eq. (17)	2	−993.58	0.87	0.13		1	7.77	663	275
			0.05	0.95		2	21.88	3105	2762
	3	−995.58	0.88	0.12	0	1	8.01	585	269
			0.21	0	0.79	2	1	1014	33
			0.002	0.07	0.93	3	14.71	3154	2835
MMPP	1	−994.28	0			1	∞	2591	2591
	2	−1016.58	-8×10^{-6}	8×10^{-6}		1	38.04	3172	3172
			12×10^{-6}	-12×10^{-6}		2	90.27	927	927
	3	−1027.46	-2×10^{-4}	8×10^{-5}	12×10^{-5}	1	0	∞	–
			16×10^{-6}	-16×10^{-6}	0	2	21.02	2973	2973
			0	-2×10^{-5}	2×10^{-5}	3	52.85	914	914

Continuous HMM ctd.

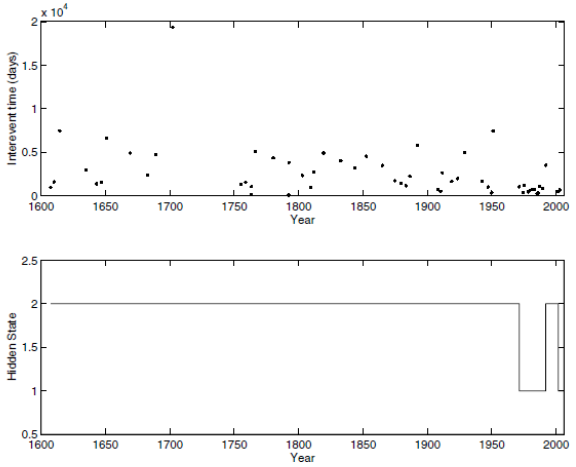

Figure 3. Mount Etna: optimal hidden path for the discrete Weibull interonset HMM.

Repose-duration HMM

Bivariate HMM coupling duration and subsequent repose ~ 'time-predictable' model

Table 7. Time-predictable models for Mount Etna.

Model	S	AIC	A				State	Sojourn (eruptions)	Repose (d) Mean	*SD*	Duration (d) Mean	*SD*
Exponential	1	−1693.00	1				1	∞	2391	2391	200	200
Eq. (19)	2	−1659.96	0.70	0.30			1	3.33	1724	1724	58	58
			0.83	0.17			2	1.20	4146	4146	575	575
	3	−1655.25	0.50	0	0.50		1	2.01	1516	1516	13	13
			0.25	0.75	0		2	4.01	1898	1898	1357	1357
			0.23	0	0.77		3	4.32	2895	2895	162	162
	4	−1658.03	1	0	0	0	1	∞	729	729	142	142
			0	0.62	0	0.38	2	2.64	1700	1700	13	13
			0	0.25	0.75	0	3	4.01	1898	1898	1356	1356
			0.05	0.26	0	0.69	4	3.24	4117	4117	171	171
Weibull	1	−1657.87	1				1	∞	2389	2520	179	313
Eq. (20)	2	−1653.96	0.94	0.06			1	15.38	2078	174	193	355
			0.61	0.39			2	1.64	7257	1851	64	6
	3	−1648.94	0.89	0	0.11		1	4.82	1489	671	14	14
			0	0.65	0.35		2	3.02	1802	2684	132	126
			0.18	0.37	0.45		3	2.08	4151	1386	484	737
	4	−1637.24	0.89	0	0.11	0	1	8.92	791	613	150	153
			0	0.62	0.38	0	2	2.65	1538	712	15	15
			0	0.40	0.36	0.24	3	1.57	4249	1306	461	684
			0.52	0	0.48	0	4	1	10797	37327	68	3

Repose-duration HMM ctd.

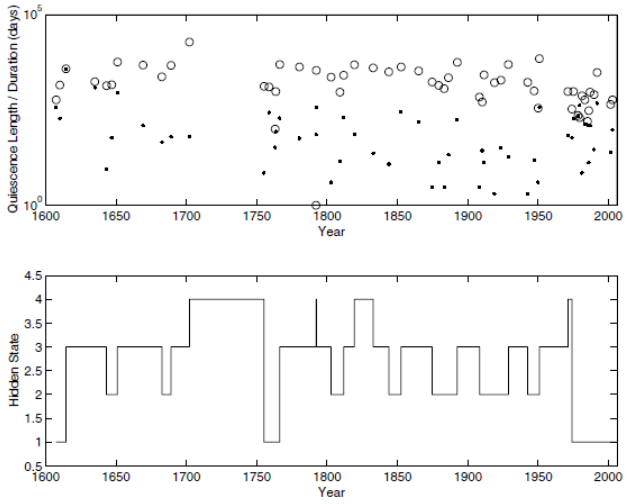

Figure 6. Mount Etna: optimal hidden path for the bivariate Weibull time-predictable HMM. Circles are repose lengths, dots durations.

Duration-repose HMM

Bivariate HMM coupling repose and subsequent duration ~ 'size-predictable' model

Table 8. Size-predictable models for Mount Etna.

Model	S	AIC	A				State	Sojourn (eruptions)	Repose (d) Mean	Repose (d) SD	Duration (d) Mean	Duration (d) SD
Exponential	1	−1691.19	1				1	∞	2391	2391	196	196
Eq. (19)	2	−1657.16	0.33	0.67			1	1.49	1190	1190	501	501
			0.31	0.69			2	3.17	2986	2986	47	47
	3	−1653.38	0.79	0	0.21		1	4.82	1930	1930	160	160
			0	0.67	0.33		2	3.02	1944	1944	1683	1683
			0.48	0	0.52		3	2.08	3437	3437	13	13
	4	−1663.74	0.45	0	0.19	0.36	1	1.81	1103	1103	222	222
			0	0.67	0.33	0	2	3.00	1941	1941	167	167
			0.35	0	0.65	0	3	2.82	2165	2165	13	13
			0.40	0	0.05	0.55	4	2.20	4396	4396	69	69
Weibull	1	−1656.03	1				1	∞	2389	2519	176	307
Eq. (20)	2	−1650.54	0.14	0.86			1	1.16	742	219	196	13
			0.07	0.93			2	13.87	2562	2682	169	317
	3	−1638.18	0	0	1		1	1	582	10	189	3
			0.02	0.98	0		2	52.1	2450	2613	110	156
			0	0.50	0.50		3	1.98	2626	1164	2467	1179
	4	−1657.00	0	0	0	1	1	1	241	475	384	25
			0.07	0.40	0.25	0.28	2	1.67	708	314	180	100
			0.07	0	0.89	0.04	3	9.37	2867	1550	185	415
			0	0.86	0	0.16	4	1.20	4077	5682	26	23

Duration-repose HMM ctd.

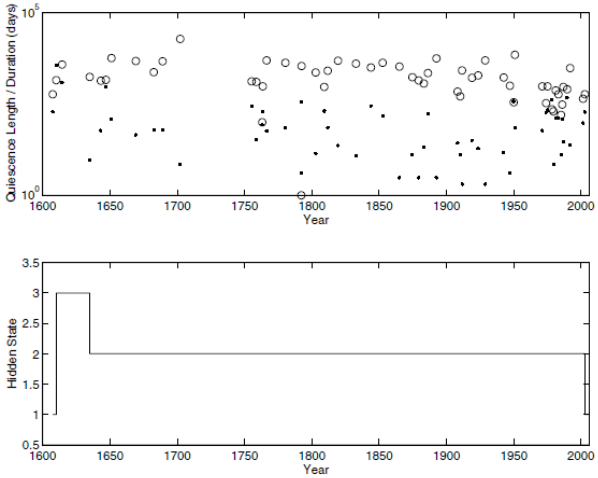

Figure 7. Mount Etna: optimal hidden path for the bivariate Weibull size-predictable HMM. Circles are repose lengths, dots durations.

Change Points

Table 12. Change points for Mount Etna flank eruptions.

Data type	Model (or other source)	States (or date range for other sources)	Change points
Onsets	Poisson, $S = 1$	Average rate	None
	Poisson, $S = 2$	Stable low rate, unstable high rate	1611, 1971, 1991
	Mulargia *et al.* (1985)	1600–1980	None
Interonset	Weibull, $S = 2$	Stable high (periodic) rate, very stable low variable rate	1971, 1991, 2001
	Mulargia *et al.* (1987)	1600–1978	1865
	Gasperini *et al.* (1990)	1978–1987	1987
	Ho (1992)	1600–1978	1702, 1759
	Marzocchi (1996)	1600–1994	(Trend)
	Sandri *et al.* (2005)	1971–2002	None
	Salvi *et al.* (2006)	1536–2001	1980
Time-predictable	Weibull, $S = 4$	High (memoryless) rate and medium (memoryless) duration Medium (periodic) rate and short (memoryless) duration Low (periodic) rate and long variable duration Very low (extremely variable) rate and short constant duration	'major' changes in 1614, 1702, 1755, 1766, 1792, 1792, 1819, 1832, 1971, 1974, and 14 others – see Section 4.4
	Wadge *et al.* (1975)	1535–1974	1610, 1669, 1759/1763
	Wadge & Guest (1981)	1971–1981	1971?
	Mulargia *et al.* (1987)	1600–1978	1670, 1750, 1950
	Gasperini *et al.* (1990)	1978–1987	None
	Sandri *et al.* (2005)	1971–2002	None
Size-predictable	Weibull, $S = 3$	Stable medium memoryless rate and medium variable duration Unstable High (periodic) rate and constant duration Low (periodic) rate and very long duration	1607, 1610, 1634, 2001, 2004

- Etna has longish periods of Poissonian behaviour, interspersed with less random periods
- Changes in regime may be more frequent than have previously been identified statistically.
- Flank eruptions appear to have a complex time-predictable character, which is compatible with transitions between an open and closed conduit system.
- The relationship between reposes and durations appears to characterize the cyclic nature of the activity.

Forecasts

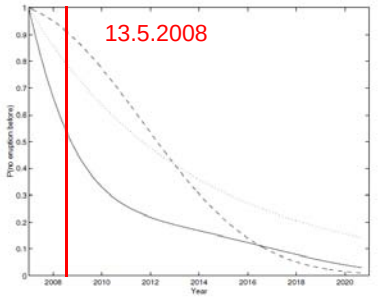

Figure 8. Mount Etna: forecast probability distribution of the next onset. Solid line = time-predictable model, dashed line = size-predictable model and dotted line = interonset model.

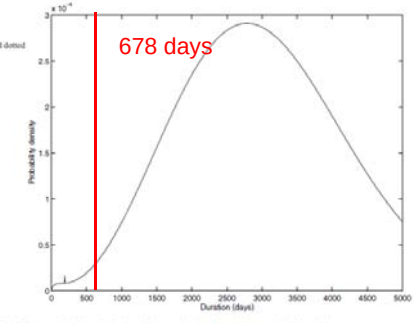

Figure 9. Mount Etna: forecast probability distribution of the next duration using the size-predictable model.

The Auckland Volcanic Field

Bebbington and Cronin (2011)

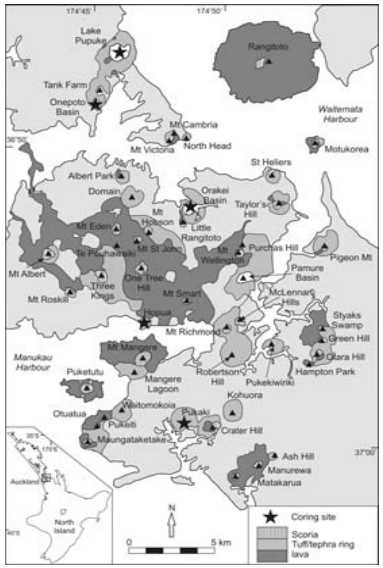

50(?) small basaltic volcanoes

young (~250,000 years)

Most recent eruption ~600 years ago

Data:

- Stratigraphy, ~33 vents constrained in at least one direction
- Age determinations
  - Paleomagnetism ~5+ vents
  - C14, ~13 vents
  - Tephrostratigraphy, 24+ tephra in 5 locations
  - Ar-Ar, ~4 vents
  - Thermoluminesence, 2 vents
  - K-Ar, unreliable due to excess Ar
- Relative geomorphology or weathering

Decreasing reliability

Also: known vent locations, reasonable volume data

Tephra Attenuation (Pupuke)

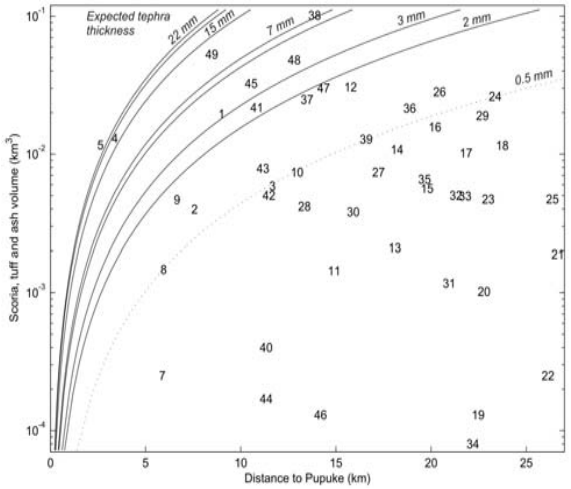

- Wind-direction (low level) assumed random throughout record
- Stratigraphy must be maintained
- Assigned tephras must be consistent with reliable dates
- Tephras must not "skip-over" sites to be only at distal areas
- All tephras must be assigned, in a **feasible** manner

$$r = -1.85V^{1/3} + \exp\left[(8.67 + 1.13\log V - \log T)/2.38\right]$$

Rhoades et al (2002)

V = volume (km³); T = thickness (cm); r = distance (km). Validated against 1977 Ukinrek Maars eruption

Palaeomagnetic Excursions

Laschamp at 40.4 ± 1.1 ka (Guillou et al, 2004)
Mono Lake at 32.4 ± 0.3 ka (Singer, 2007).
- Both are considered to last approximately 1 ka.

Cassidy and Locke (2009, 2010) suggest:

A) In ML [within 0.1ka?] [TH at slightly different time?]

D) Identical magnetism - within 0.1ka?

Stratigraphy:
(Waitomokoia > Pukeiti > Otuataua)
- Waitomokoia much older than estimated

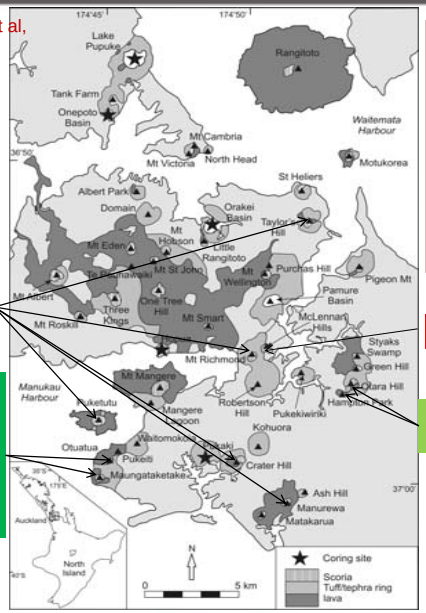

E) Others have normal magnetism, cannot be in excursion, except possibly:
Tank Farm
Onepoto
St Heliers
Orakei Basin
Hopua
Pukaki
Little Rangitoto
Pukeiti
(Cassidy, pers. comm.).

B) In Laschamp

C) Contemporaneous - within 0.1ka

A Monte Carlo sample of age-orderings

By reverse engineering the tephra dispersal, Bebbington and Cronin (2011) constructed an algorithm to produce ***feasible*** age-orderings.

Laschamp magnetic excursion →

This has **no apparent spatio-temporal structure**, although there is plenty of both temporal and spatial structure

Mono Lake magnetic excursion ↗

Name	Mean Age (ka)	Age Error (ka)	Min Order	Max Order
Onepoto Basin	248.4	27.8	1	7
Albert Park	229.8	39.5	1	7
.....	.....	.....	.....	.....
St Heliers	185.0	52.8	2	9
Te Pouhawaiki	152.9	70.3	1	34
.....	.....	.....	.....	.....
Mt St John	54.8	4.6	10	13
Maungataketake	41.4	0.4	13	15
Otuataua	41.4	0.4	14	16
McLennan Hills	40.1	1.2	13	16
One Tree Hill	34.9	0.7	16	18
.....	.....	.....	.....	.....
Hopua Basin	32.3	0.4	19	26
Puketutu	31.9	0.3	22	27
Wiri Mountain	31.9	0.3	21	28
Mt Richmond	31.7	0.3	21	28
Taylors Hill	31.7	0.3	21	28
Crater Hill	31.6	0.3	23	28
North Head	31.2	0.1	27	29
.....	.....	.....	.....	.....

Time-Varying Eruption Rate

Interevent time distribution

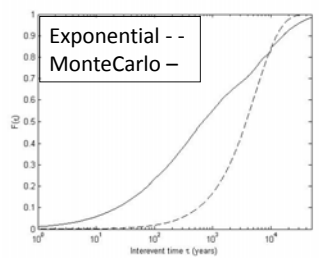

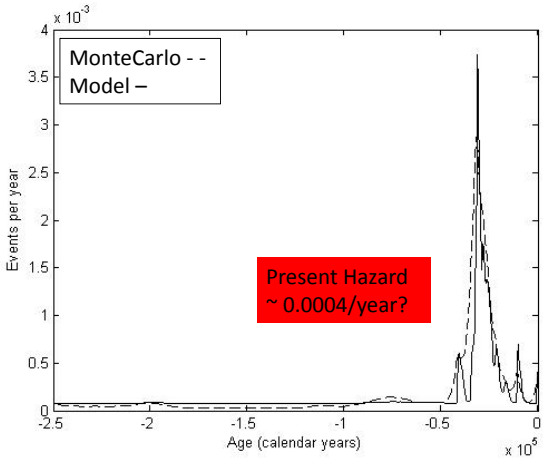

Excess of both short and long reposes
➢ 'self-exciting' model

$$\lambda(t) = \mu + \frac{\nu}{\sigma}\sqrt{\frac{2}{\pi}}\sum_{j:t_j<t}\exp\left(-\frac{(t-t_j)^2}{2\sigma^2}\right)$$

Spatial Structure, Second Order Analysis

- **azimuths of sequential pairs shows a tendency to AVOID alignments**

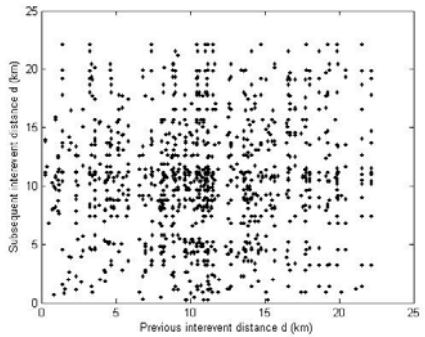

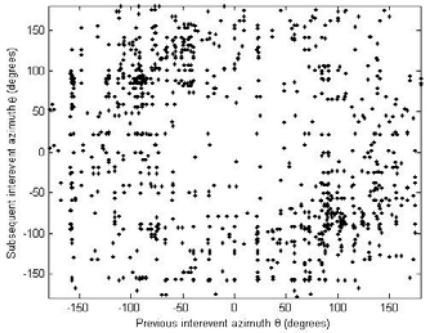

Spatial Likelihood

- **Kernel estimate of spatial probability (Connor and Connor 2009)**
  - **Ruaumoko location not relatively unlikely ☺**

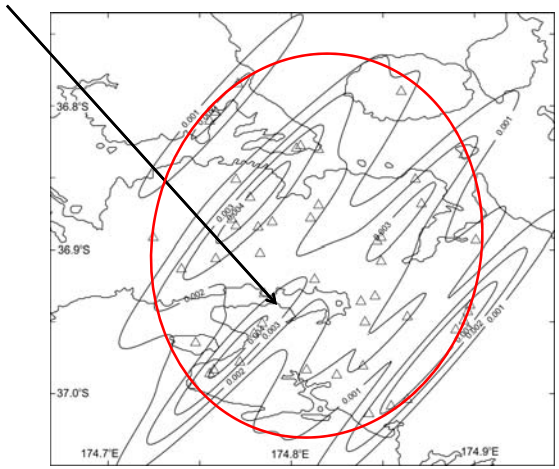

Elliptical boundary (Sporli and Eastwood, 1997)

Models for E/Q Triggering of Volcanic Eruptions

Bebbington and Marzocchi (2011)

Linde and Sacks (1998)

Remote dynamical triggering of eruptions due to passing of seismic waves.

8 cases post-1900

Peturbation' models allow for delayed triggering (Marzocchi et al, 2002)

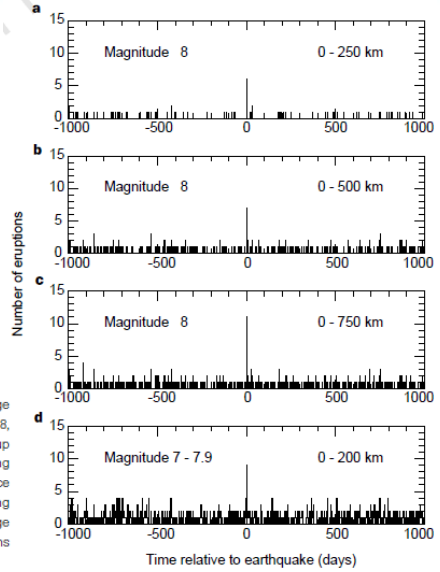

Figure 1 Histograms of number of eruptions occurring within ±1,000 days of large earthquakes. In **a**, **b** and **c**, the eruptions, following earthquakes of magnitude >8, are grouped in 1-day bins; **a**, **b** and **c** are for earthquake–eruption distances of up to 250 km, 500 km and 750 km, respectively. The large peak for the bin following the earthquake is evidence for a triggering effect, although there is no evidence for triggering in the distance range 250–500 km. In **d**, the eruptions following earthquakes of magnitude 7–7.9 are grouped in 2-day bins for the distance range 0–200 km. Most of these eruptions are at distances >100 km. All other time bins display expected random values.

E/Qs and Volcanoes of Indonesia

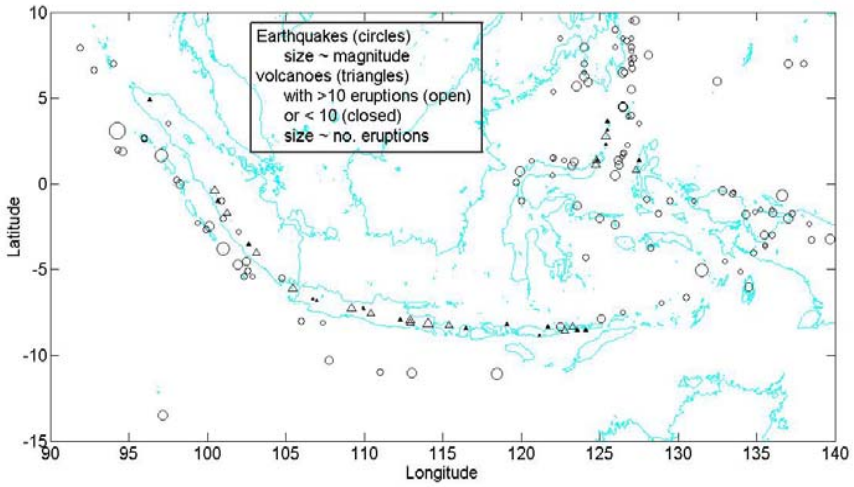

E/Qs and Volcanoes of Indonesia – Completeness?

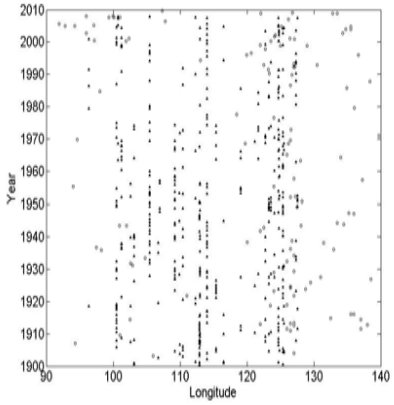

Figure 2. Time and location (longitude) of earthquakes (circles) and eruptions (triangles).

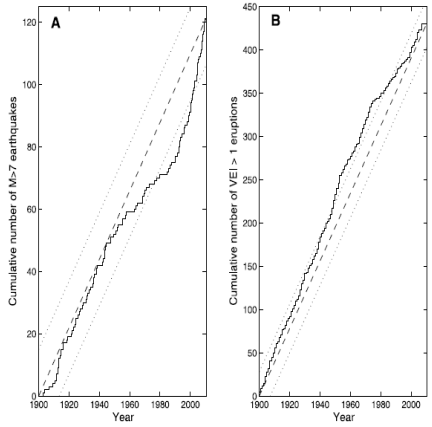

Figure 3. (a) Cumulative numbers of earthquakes with $M \geq 7$ and (b) eruptions with VEI ≥ 2 at volcanoes with at least three eruptions from 1900 to 2010. The dotted lines indicate the 95% Kolmogorov-Smirnov limits.

Baseline stochastic models

Last eruption: volume v, at time u

- Poisson process (PP), $\lambda(t) = \lambda_0$
- Weibull renewal model (WRM),
  $\lambda(t-u) = \alpha\beta^{\alpha}(t-u)^{\alpha-1}$
- Generalized time predictable model (GTPM)

$$\lambda(t-u|v) = \frac{\frac{1}{(t-u)\sigma\sqrt{2\pi}}\exp\left\{-0.5\left[\frac{\log(t-u)-\alpha-\beta v}{\sigma}\right]^2\right\}}{1-\Phi\left[\frac{\log(t-u)-\alpha-\beta v}{\sigma}\right]}$$

(Marzocchi and Zaccarelli, 2006)

- Volume History Model (VHM)

$\lambda(t) = \exp\{\alpha + \nu[\rho t - V(t)]\}$, where V(t) is the cumulative volume erupted prior to time t

(Bebbington, 2008)

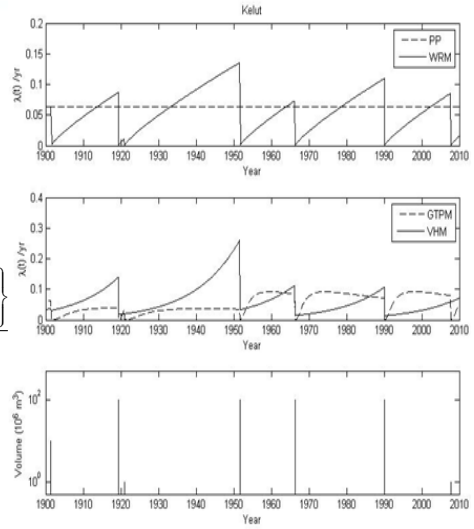

Incorporating E/Q Triggering

Multiply baseline point process intensity by a triggering term:

$$\lambda_i(t) = \lambda_i^{(B)}(t)\lambda_i^{(T)}(t)$$
$$= \lambda_i^{(B)}(t)\left\{1 + \sum_{j:s_j<t}\exp\left[-a(t-s_j) - b\log r_{ij} + cm_j\right]\right\}$$

where the jth earthquake occurs at time s_j , j =1,...,J, a distance r_{ij} from volcano i, and has magnitude m_j

- Model without triggering nested
- Triggering decays exponentially with time
- Triggering decays with distance as a power law
  (static stress ~r^{-3} , dynamic stress ~$r^{-1.66}$)
- Exponential increase with magnitude commensurate with increase in action radius proportional to rupture length (Lemarchand and Grasso, 2007)

Best Model (by AIC)

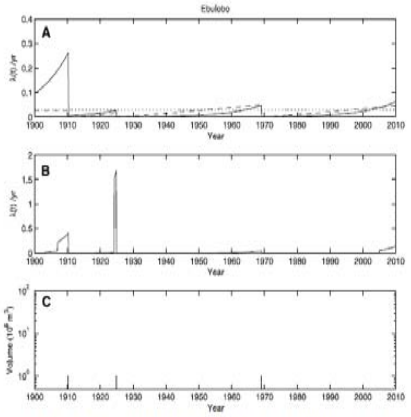

Figure 9. Ebulobo volcano. (a) Fitted conditional intensities (nontriggered): Poisson (dotted), Weibull renewal (dashed), and volume history (solid). (b) Fitted conditional intensity for the triggered volume history model (note difference in vertical scale from Figure 9a); the timing of relevant earthquakes are indicated by upward jumps. (c) Time size (VEI) plot of eruptions.

'Best' model independent of number of eruptions, location of volcano

Model	No. Parameters	No. Volcanoes
Poisson	1	10
Weibull Renewal	2	4
GTPM	3	4
Volume History	3	10
Poisson w. E/Q triggering	4	0
Weibull Renewal w. E/Q triggering	5	0
Volume History w. E/Q triggering	6	7

Are the 7 (out of 35) 'triggered' volcanoes due to more than random chance?
- As our models are nested, we can use a likelihood ratio test.

Improvement relative to Poisson process

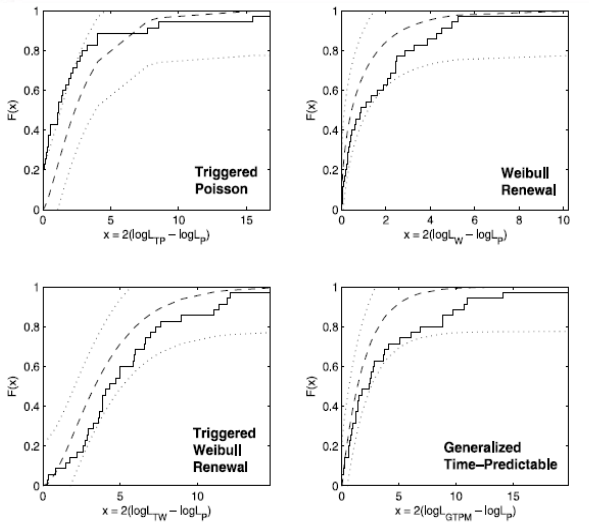

Figure 4. AIC improvement relative to the Poisson process. The solid line is the empirical (35 volcanoes) distribution of $\Delta AIC + 2(k-1)$, where k is the number of parameters in the given model and ΔAIC is the difference in AIC from the Poisson process. The theoretical χ^2_{k-1} distribution is the dashed line, and the dotted lines are the 95% Kolmogorov-Smimov limits.

Volume dependence and triggering

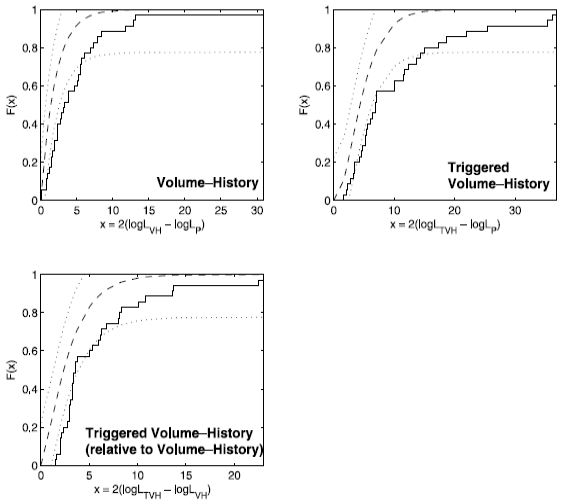

Figure 5. (top) AIC improvement relative to the Poisson process. The solid line is the empirical (35 volcanoes) distribution of Δ AIC + 2(k − 1), where k is the number of parameters in the given model and ΔAIC is the difference in AIC from the Poisson process. The theoretical χ^2_{k-1} distribution is the dashed line, and the dotted lines are the 95% Kolmogorov-Smimov limits. (bottom) The same for the triggered volume history model relative to the volume history model.

Volume dependence and triggering – Individual Volcanoes

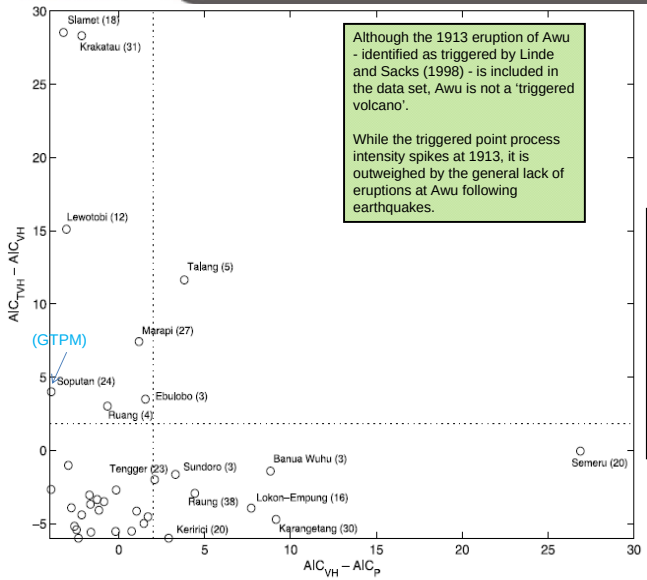

Although the 1913 eruption of Awu - identified as triggered by Linde and Sacks (1998) - is included in the data set, Awu is not a 'triggered volcano'.

While the triggered point process intensity spikes at 1913, it is outweighed by the general lack of eruptions at Awu following earthquakes.

- While approximately 0.3–0.4% of eruptions are directly triggered (Linde and Sacks 1998), here 25% occur at volcanoes with a statistically significant tendency to triggering.
- With the exception of Ruang, all the triggered volcanoes possess multiple vents.

Figure 6. AIC improvement from incorporating volume history and then earthquake triggering. The dotted lines indicate the 5% level of significance. The number of eruptions follows the volcano name.

Interpretation of Triggering – Clock Advance

- In order for triggering to be recognized, we must account for the erupted-volume history of the volcano.
- Size of eruption appears to be independent of whether it was triggered.
- The 2005 eruption of Talang has a spike derived from the 2004 Sumatra earthquake (cf. Walter and Amelung, 2007), as do subsequent eruptions - from the M>7 aftershocks.
- We conclude that triggering affects volcanoes that were 'ready' to erupt – a form of 'clock advance' familiar in the earthquake literature.

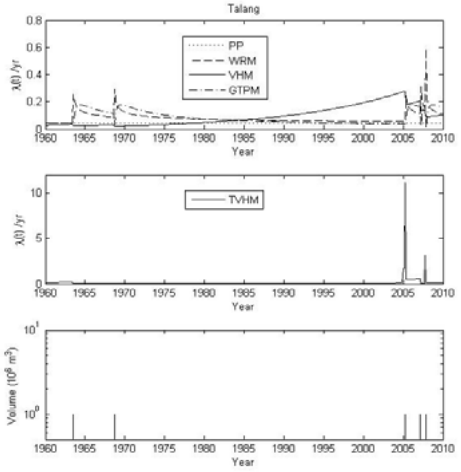

References

Bebbington M (2007) Identifying volcanic regimes using hidden Markov models. Geophys J Int 171, 921-942

Bebbington MS (2008) Incorporating the eruptive history in a stochastic model for volcanic eruptions, J Volcanol Geotherm Res 175, 325-333

Bebbington M (2010) Trends and clustering in the onsets of volcanic eruptions. J Geophys Res 115, B01203, doi:10.1029/2009JB006581

Bebbington M, Cronin SJ (2011) Spatio-temporal hazard estimation in the Auckland Volcanic Field, New Zealand, with a new event-order model. Bull Volcanol 73, 55-72.

Bebbington MS, Harte DS (2001) On the statistics of the linked stress release process. J Appl Probab 38A, 176-187.

Bebbington MS, Harte DS (2003) The linked stress release model for spatio-temporal seismicity: formulations, procedures and applications. Geophys J Int 154, 925-946

Bebbington MS, Lai CD (1996) On nonhomogeneous models for volcanic eruptions, Math Geol 28, 585-600

Bebbington MS, Marzocchi W (2011) Stochastic models for earthquake triggering of volcanic eruptions. J Geophys Res 116, B05204, doi:10.1029/2010JB008114

Connor CB, Connor LJ (2009) Estimating spatial density with kernel methods. In: Connor CB, Chapman NA, Connor LJ (eds) Volcanic and tectonic hazard assessment for nuclear facilities. Cambridge University Press, Cambridge, UK, pp 346–368

Guttorp P, Thompson ML (1991) Estimating second-order parameters of volcanicity from historical data. JASA 86, 578-583

Lemarchand N, Grasso J-R (2007) Interactions between earthquakes and volcanic activity, Geophys Res Lett 34, L24303

Lindqvist BH, Elvebakk G, Heggland K (2003) The trend-renewal process for statistical analysis of repairable systems. Technometrics 45, 31– 44.

Lu C, Harte DS, Bebbington MS (1999) A linked stress release model for historical earthquakes from Japan: Implications for coupling among major seismic regions. Earth Planets Space 51, 907-916.

Marzocchi W, Zaccarelli L (2006) A quantitative model for the time-size distribution of eruptions, J Geophys Res 111, B04204

Marzocchi W, Casarotti E, Piersanti A (2002) Modeling the stress variations induced by great earthquakes on the largest volcanic eruptions of the 20th century, J Geophys Res 107, 2320

Rhoades DA, Dowrick DJ, Wilson CJN (2002) Volcanic hazard in New Zealand: scaling and attenuation relations for tephra fall deposits from Taupo Volcano, Nat Hazards 26, 147–174

Sporli KB, Eastwood VR (1997) Elliptical boundary of an intraplate volcanic field, Auckland, New Zealand. J Volcanol Geotherm Res 79, 169-179

Turner M, Cronin S, Bebbington M, Platz T (2008) Developing a probabilistic eruption forecast for dormant volcanos; a case study from Mt Taranaki, New Zealand. Bull Volcanol 70, 507–515

Turner M, Bebbington M, Cronin S, Stewart RB (2009) Merging eruption datasets: building an integrated Holocene eruptive record of Mt Taranaki. Bull Volcanol 71, 903–918

Walter TR, Amelung F (2007) Volcanic eruptions following M≥9 megathrust earthquakes: Implications for the Sumatra-Andaman volcanoes, Geology 35, 539-542